Mechanistic Insights into Hsp104 Potentiation*

Mariana P. Torrente[‡1], Edward Chuang[‡§2], Megan M. Noll[‡], Meredith E. Jackrel[‡3], Michelle S. Go[‡4], and James Shorter[‡§5]

From the ‡Department of Biochemistry and Biophysics and the §Pharmacology Graduate Group, Perelman School of Medicine, University of Pennsylvania, Philadelphia, Pennsylvania 19104

Potentiated variants of Hsp104, a protein disaggregase from yeast, can dissolve protein aggregates connected to neurodegenerative diseases such as Parkinson disease and amyotrophic lateral sclerosis. However, the mechanisms underlying Hsp104 potentiation remain incompletely defined. Here, we establish that 2–3 subunits of the Hsp104 hexamer must bear an A503V potentiating mutation to elicit enhanced disaggregase activity in the absence of Hsp70. We also define the ATPase and substrate-binding modalities needed for potentiated Hsp104[A503V] activity in vitro and in vivo. Hsp104[A503V] disaggregase activity is strongly inhibited by the Y257A mutation that disrupts substrate binding to the nucleotide-binding domain 1 (NBD1) pore loop and is abolished by the Y662A mutation that disrupts substrate binding to the NBD2 pore loop. Intriguingly, Hsp104[A503V] disaggregase activity responds to mixtures of ATP and adenosine 5′-(γ-thio)-triphosphate (a slowly hydrolyzable ATP analogue) differently from Hsp104. Indeed, an altered pattern of ATP hydrolysis and altered allosteric signaling between NBD1 and NBD2 are likely critical for potentiation. Hsp104[A503V] variants bearing inactivating Walker A or Walker B mutations in both NBDs are inoperative. Unexpectedly, however, Hsp104[A503V] retains potentiated activity upon introduction of sensor-1 mutations that reduce ATP hydrolysis at NBD1 (T317A) or NBD2 (N728A). Hsp104[T317A/A503V] and Hsp104[A503V/N728A] rescue TDP-43 (TAR DNA-binding protein 43), FUS (fused in sarcoma), and α-synuclein toxicity in yeast. Thus, Hsp104[A503V] displays a more robust activity that is unperturbed by sensor-1 mutations that greatly reduce Hsp104 activity in vivo. Indeed, ATPase activity at NBD1 or NBD2 is sufficient for Hsp104 potentiation. Our findings will empower design of ameliorated therapeutic disaggregases for various neurodegenerative diseases.

Protein misfolding and aggregation are associated with a wide variety of diseases, ranging from type II diabetes (1, 2) to neurodegenerative diseases, such as fatal familial insomnia (3, 4), Parkinson disease, and amyotrophic lateral sclerosis (ALS) (5–7). In Parkinson disease patients, α-synuclein (α-syn)[6] forms toxic soluble oligomers as well as amyloid structures that accumulate in Lewy bodies and contribute to the death of dopaminergic neurons (8–12). Similarly, toxic soluble oligomers and cytoplasmic inclusions of TDP-43 or FUS are associated with ALS and frontotemporal dementia (13–20). These misfolded protein conformers are recalcitrant and represent a colossal roadblock in the treatment of these diseases.

Hsp104 is a 102-kDa AAA+ ATPase (21) from Saccharomyces cerevisiae capable of dissolving disordered protein aggregates as well as dismantling amyloid fibrils and toxic soluble oligomers (22–33). It assembles into a homohexameric barrel structure with a central channel (34–39). Hsp104 processes protein aggregates by directly translocating substrates either partially or completely through this channel (35, 36, 40–46). Hsp104 encompasses an N-terminal domain, two nucleotide-binding domains (NBD1 and NBD2), a coiled-coil middle domain (MD), and a C-terminal domain important for oligomerization (Fig. 1A) (47). Both NBDs contain Walker A and Walker B motifs that are critical for nucleotide binding and hydrolysis, respectively (48). ATP hydrolysis takes place primarily at NBD1, whereas NBD2 has a nucleotide-dependent oligomerization function (29, 34, 49–52).

Remarkably, Hsp104 can remodel amyloid substrates alone, without the aid of any other chaperones (22, 24, 26, 31, 33, 45, 53–56). However, to disaggregate amorphous protein aggregates, Hsp104 usually needs to collaborate with the Hsp110, Hsp70, and Hsp40 chaperone system (23, 26, 30, 32, 57). Moreover, small heat shock proteins such as Hsp26 can enhance disaggregase activity further (30, 57–59). In vitro, mixtures of ATP and ATPγS (a slowly hydrolyzable ATP analogue) enable Hsp104 to dissolve amorphous aggregates in the absence of Hsp70 and Hsp40 (26, 35, 60, 61).

Wild-type (WT) Hsp104 can resolve α-syn oligomers and fibrils, but very high Hsp104 concentrations are required (26, 31, 32). Hsp104 has limited disaggregase activity against

[6] The abbreviations used are: α-syn, α-synuclein; FUS, fused in sarcoma; ATPγS, adenosine 5′-(γ-thio)triphosphate; NBD, nucleotide-binding domain; TDP-43, TAR DNA-binding protein 43; MD, middle domain.

Mechanistic Insights into Hsp104 Potentiation

TDP-43 and FUS fibrils (62, 63). Recently, we have engineered potentiated Hsp104 variants that mitigate TDP-43, FUS, and α-syn misfolding (62–67). Missense mutations at disparate but specific positions in the MD or the small domain of NBD1 (immediately C-terminal to the MD) resulted in potentiated Hsp104 variants (62, 67). Potentiating mutations in the MD obviate any absolute requirement for Hsp70 in disaggregation of amorphous aggregates and typically (under physiological salt conditions) enhance Hsp104 ATPase activity (62, 67). Potentiated Hsp104 variants also display accelerated substrate translocation, enhanced unfoldase activity, and enhanced amyloid-remodeling activity (45, 62). They can also recognize shorter unfolded tracts in client proteins compared with Hsp104 (63). Hsp104^{A503V} has been previously established as a potentiated Hsp104 variant able to ameliorate the toxicity arising from the aggregation of WT or disease-linked forms of α-syn, FUS, and TDP-43 in yeast (62, 63). Hsp104^{A503V} hexamers also display enhanced plasticity and are more resistant to defective subunits than Hsp104 (62). However, Hsp104^{A503V} is more sensitive than Hsp104 to suramin, a small molecule inhibitor of Hsp104 ATPase activity (68). Interestingly, two potentiated Hsp104 variants, Hsp104^{A503S} and Hsp104$^{Y257F/A503V/Y662F}$, rescue neurodegeneration in the metazoan nervous system and hold promise as possible treatments for neurodegenerative disease (62, 66).

Despite these advances, the molecular mechanisms underlying the potentiation of Hsp104 are incompletely understood. The N-terminal domain of Hsp104 is critical for Hsp104 potentiation, as is motif 1 (helix 1 and a portion of helix 2) of the MD (35, 47, 67). Thus, deletion of these large regions precludes potentiation (35, 67). However, beyond these domain requirements, little else is known. Here, we explore how many A503V subunits are needed per hexamer to enable enhanced activity. We also determine which Hsp104 ATPase and substrate-binding modalities are important for potentiation both *in vitro* and *in vivo*. The mechanistic insights gleaned from our studies will enable further development of potentiated Hsp104 variants as therapeutics for various neurodegenerative diseases.

Experimental Procedures

Materials—All chemicals were purchased from Sigma-Aldrich unless otherwise specified. Creatine kinase was purchased from Roche Applied Science. Firefly luciferase was purchased from Sigma-Aldrich. Luciferase assay reagent was purchased from Promega (Madison, WI). Hsp70 (Hsp72) and Hsp40 Hdj1 were purchased from Enzo Life Sciences (Farmingdale, NY).

Protein Expression and Purification—Sixteen Hsp104 variants: Hsp104, Hsp104^{Y257A}, Hsp104^{T317A}, Hsp104^{A503V}, Hsp104^{Y662A}, Hsp104^{N728A}, Hsp104$^{K218T/K620T}$, Hsp104$^{E285Q/E687Q}$, Hsp104$^{Y257A/Y662A}$, Hsp104$^{Y257A/A503V}$, Hsp104$^{T317A/A503V}$, Hsp104$^{Y662A/A503V}$, Hsp104$^{N728A/A503V}$, Hsp104$^{K218T/A503V/K620T}$, Hsp104$^{E285Q/A503V/E687Q}$, and Hsp104$^{Y257A/A503V/Y662A}$ were purified as reported previously (52, 61, 69). Briefly, untagged Hsp104 was transformed into BL21-DE3 RIL cells (Agilent Technologies, Santa Clara, CA). Expression was induced at an A_{600} of 0.4–0.6 with 1 mM isopropyl 1-thio-β-D-galactopyranoside for 15–18 h at 15 °C. Cells were harvested via centrifu-

gation (4,000 rpm, 4 °C, 20 min), resuspended in lysis buffer (50 mM Tris-HCl, pH 8.0, 10 mM MgCl$_2$, 2.5% glycerol (w/v), 2 mM β-mercaptoethanol (Bio-Rad), 5 μM pepstatin A, and 1 Mini-complete EDTA free protease tablet per 50 ml (Roche Applied Science), and lysed by sonication. Cell debris was removed via centrifugation at 16,000 rpm at 4 °C for 20 min. The supernatant was applied to Affi-Gel Blue resin (Bio-Rad). Supernatant and resin were rotated at 4 °C for 4 h. Resin was then washed with wash buffer (50 mM Tris-HCl, pH 8.0, 10 mM MgCl$_2$, 100 mM KCl, 2.5% glycerol (w/v), 2 mM β-mercaptoethanol). Hsp104 was eluted with high salt buffer (wash buffer plus 1 M KCl). Hsp104 was then further purified by ResourceQ anion exchange chromatography using running buffer Q (20 mM Tris-HCl, pH 8.0, 0.5 mM EDTA, 5 mM MgCl$_2$, 50 mM NaCl) and eluted with a linear gradient of buffer Q+ (20 mM Tris-HCl, pH 8.0, 0.5 mM EDTA, 5 mM MgCl$_2$, 1 M NaCl). Eluate was exchanged into storage buffer (40 mM HEPES-KOH, pH 7.4, 150 mM KCl, 20 mM MgCl$_2$, 10% glycerol, 1 mM DTT), snap-frozen, and stored at −80 °C. High salt storage buffer (40 mM HEPES-KOH, pH 7.4, 500 mM KCl, 20 mM MgCl$_2$, 10% glycerol, 1 mM DTT) was used for storage of Hsp104^{A503V} and all other Hsp104 variants containing this mutation.

ATPase Assay—WT or mutant Hsp104 (0.25 μM monomer) in ATPase buffer (20 mM HEPES-KOH, pH 7.4, 20 mM NaCl, and 10 mM MgCl$_2$) was incubated for 10 min at 25 °C in the presence of ATP (1 mM) as noted (52). ATPase activity was assessed by the release of inorganic phosphate determined by using a malachite green phosphate detection kit (Innova Biosciences, Cambridge, UK).

Luciferase Disaggregation Assays—Luciferase reactivation was performed as described (23, 61). To assemble aggregates, firefly luciferase (50 μM) in luciferase refolding buffer (25 mM HEPES-KOH, pH 7.4, 150 mM potassium acetate, 10 mM magnesium acetate, 10 mM DTT) with 6 M urea was incubated at 30 °C for 20 min. Luciferase was then rapidly diluted 100-fold into luciferase refolding buffer, divided into 100-μl aliquots, snap-frozen in liquid N$_2$, and stored at −80 °C. For reactivation assays, aggregated luciferase (50 nM) was incubated with Hsp104 (1 μM hexamer) plus 5 mM ATP (or the indicated ATPγS and ATP ratio amounting to the same total) and an ATP regeneration system (10 mM creatine phosphate, 0.5 μM creatine kinase (Roche Applied Science), 0.1 mM ATP) for 90 min at 25 °C. For some assays, Hsp70 (1 μM) and Hsp40 (1 μM; Enzo Life Sciences) were added. Luciferase activity was assessed by luminescence measured on a Safire^2 microplate reader (Tecan, Männedorf, Switzerland).

Subunit Doping Assay—Hsp104 was mixed with Hsp104^{A503V} in varying ratios to give a total concentration of 0.167 μM Hsp104 hexamer, and the luciferase reactivation experiments were performed as described above. Hsp70 and Hsp40 were omitted for these experiments such that WT Hsp104 was inactive. Thus, under these conditions, we are certain that if the number of WT subunits per hexamer exceeds five, then the hexamer is inactive. We employed the approach of Reinstein and colleagues (70) to simulate the distribution of Hsp104 and Hsp104^{A503V} subunits within a given population of Hsp104 hexamers as described (26, 61, 62, 70). Thus, we employed the binomial distribution,

$$P(x) = \binom{n}{x} p^x (1-p)^{n-x} \qquad \text{(Eq. 1)}$$

where P is the probability that a hexamer (therefore, $n = 6$) contains x WT subunits, and p is the probability that a WT subunit is incorporated (26, 61, 62, 70). Experiments demonstrated that WT and A503V subunits have a similar probability of being incorporated into a hexamer (26, 62). Consequently, p is calculated as the molar ratio of WT and A503V protein present.

$$p = \frac{Hsp104}{(Hsp104 + Hsp104_{A503V})} \qquad \text{(Eq. 2)}$$

Therefore, for any specified percentage of WT subunits, the probability distribution of Hsp104^{A503V} hexamers containing zero, one, two, three, four, five, or six WT subunits can be derived (Fig. 1*B*) (26, 61, 62, 70). Activity *versus p* plots could then be generated, assuming each A503V subunit makes an equal contribution to the total activity (one-sixth per subunit) (Fig. 1*C*) (26, 61, 62, 70). Consequently, if subunits within the Hsp104^{A503V} hexamer operate independently, then activity should decline in a linear manner upon incorporation of WT subunits (26, 61, 62, 70). Conversely, if subunits are coupled, then a specific number of WT subunits will be sufficient to eliminate activity (26, 61, 62, 70). Thus, zero activity is assigned to hexamers that are in breach of a specific threshold number of WT subunits (26, 61, 62, 70). In this way, we can generate activity *versus p* plots if we assume that 1 or more, 2 or more, 3 or more, 4 or more, or 5 or more WT subunits are required to eliminate activity (26, 61, 62, 70).

To further model the observed inhibitory effect of WT Hsp104 subunits on Hsp104^{A503V} activity, we employed the binomial distribution as above but imposed an additional rule whereby WT subunits repress the activity of adjacent A503V subunits by a factor of r (26, 35, 62, 71). Thus, we scored each subunit-subunit interface of every possible heterohexamer in each possible configuration as follows: interfaces were scored as 1/6 if at an A503V:A503V junction, $r/6$ if at an A503V:WT junction, or 0 if at a WT:WT junction (26, 62). Activity was then normalized to the predicted heterohexamer population as defined by the binomial distribution above (Fig. 1*B*) (26, 59).

Yeast Strains, Media, and Plasmids—All yeasts were W303a-$\Delta hsp104$ (*MATa, can1-100, his3-11,15, leu2-3,112, trp1-1, ura3-1, ade2-1*) (72). Yeasts were grown in synthetic medium lacking the appropriate components. Medium was supplemented with 2% glucose, raffinose, or galactose. Vectors encoding TDP-43, FUS, and α-syn (pAG303GAL-TDP-43, pAG303GAL-FUS, and pAG303GAL-α-syn-GFP, respectively) were from A. Gitler (73–75). pRS416GAL-Hsp104 variants have been described previously (62). Hsp104 mutations were generated using QuikChange site-directed mutagenesis (Agilent Technologies, Santa Clara, CA) and confirmed by DNA sequencing.

Yeast Transformation and Spotting Assays—Yeast were transformed according to standard protocols using polyethylene glycol and lithium acetate (76). For the spotting assays, yeasts were grown to saturation overnight in raffinose supplemented dropout medium at 30 °C. Cultures were serially diluted 5-fold and spotted in duplicate onto synthetic dropout medium containing glucose or galactose. Plates were analyzed after growth for 2–3 days at 30 °C.
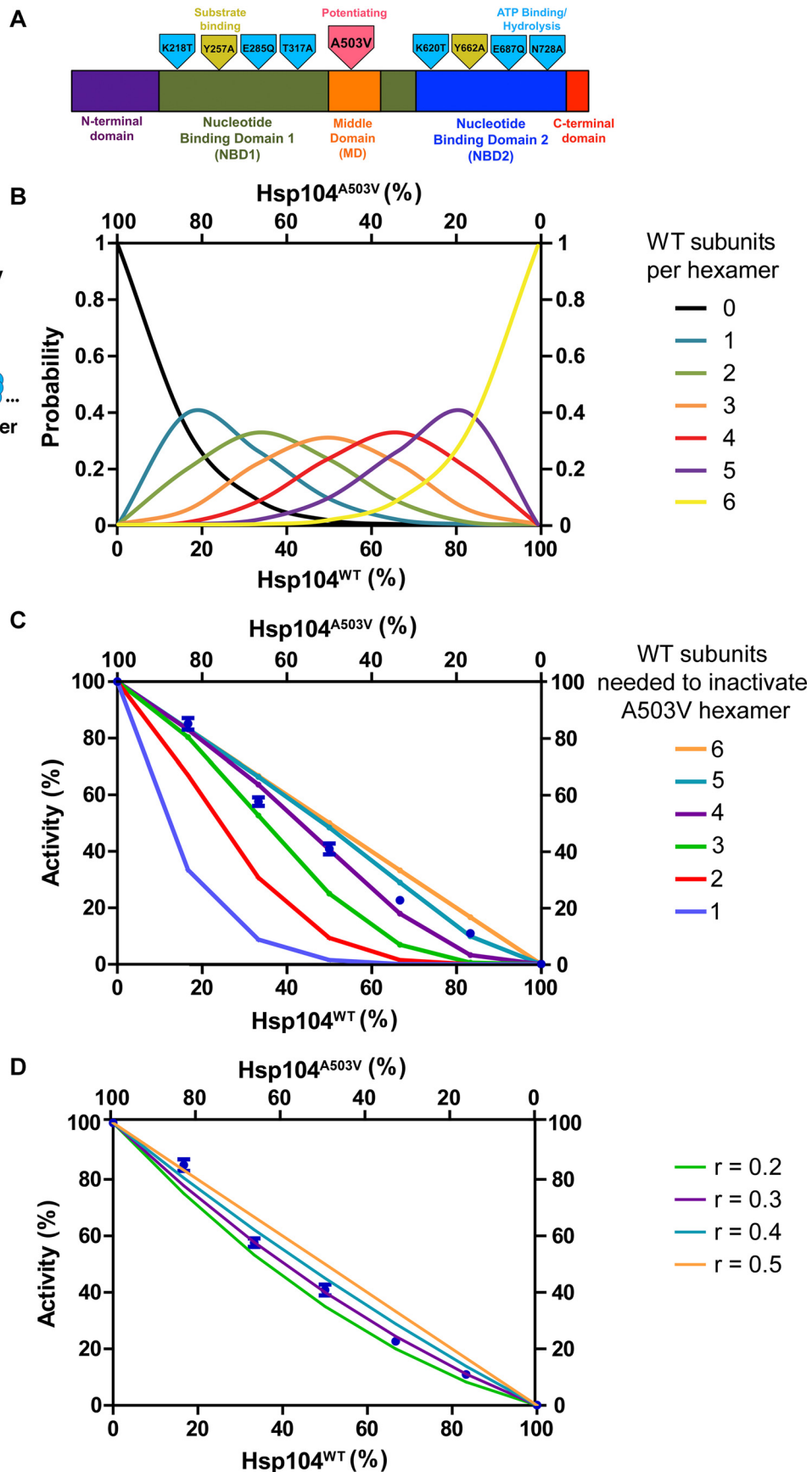
Western Blotting—Yeasts were grown and induced in galactose-containing medium for 5 h (TDP-43 and FUS) or 8 h (α-syn-GFP). Cultures were normalized to an optical density of 0.6; 6 ml of cells were then harvested and treated with 0.2 M NaOH for 5 min at room temperature. The resulting cell pellets were resuspended in 100 μl of 1× SDS sample buffer and boiled. Cell lysates were separated using SDS-PAGE (4–20% gradient; Bio-Rad) and then transferred to a PVDF membrane (EMD Millipore, Billerica, MA). Membranes were blocked using LI-COR blocking buffer for 1 h at room temperature. Primary antibody incubations were performed at 4 °C overnight. Antibodies used were as follows: rabbit anti-GFP polyclonal (Sigma-Aldrich, catalog no. G1544), rabbit anti-TDP-43 polyclonal (Proteintech (Chicago, IL), catalog no. 10782-2-AP), rabbit anti-FUS polyclonal (Bethyl Laboratories (Montgomery, TX), catalog no. A300-302A), rabbit anti-Hsp104 polyclonal (Enzo Life Sciences, catalog no. ADI-SPA-1040-F), and mouse anti-3-phosphoglycerate kinase monoclonal (Novex (Frederick, MD), catalog no. 459250). Blots were processed using goat anti-mouse and anti-rabbit secondary antibodies from LI-COR Biosciences (Lincoln, NE) and imaged using an Odyssey Fc Imaging system (LI-COR Biosciences).

Results

Hsp104 Hexamers Must Contain 2–3 A503V Subunits for Enhanced Disaggregase Activity—To gain insight into the mechanism of Hsp104 potentiation, we focused on Hsp104^{A503V} (Fig. 1*A*), which is among the strongest suppressors of α-syn, FUS, and TDP-43 toxicity in yeast (62, 63, 67). First, we explored the effects of WT Hsp104 subunits on the disaggregase activity of Hsp104^{A503V} hexamers. To do so, we exploited the strict requirement of Hsp104 for Hsp70 and Hsp40 to reactivate luciferase trapped in disordered aggregates in the presence of ATP (23, 26). In the absence of Hsp70 and Hsp40, Hsp104 reactivation activity was abolished (Fig. 1*C*) (23, 26). By contrast, Hsp104^{A503V} displayed robust luciferase reactivation activity in the absence of Hsp70 and Hsp40 (Fig. 1*C*) (62). Thus, under these conditions, we are certain that if the number of WT subunits per Hsp104 hexamer exceeds five, then the hexamer is inactive. To determine how many A503V subunits per hexamer are required to elicit disaggregase activity in the absence of Hsp70 and Hsp40, we employed a mutant subunit doping strategy (26, 70). Here, subunits were mixed to generate heterohexamer ensembles according to the binomial distribution (Fig. 1*B*) (26, 70). We have previously demonstrated that Hsp104 and Hsp104^{A503V} assemble into dynamic hexamers that rapidly exchange subunits, ensuring statistical incorporation of individual subunits (Fig. 1*B*) (26, 62). By applying different heterohexamer ensembles composed of Hsp104 and Hsp104^{A503V} subunits to reactivate disordered luciferase aggregates, we can obtain a measure of how many A503V subunits per hexamer are required for disaggregase activity in the absence of Hsp70 (Fig. 1, *B* and *C*) (26, 29, 61, 62, 70).

We assembled different heterohexamer ensembles of Hsp104^{A503V} and Hsp104^{WT} subunits (Fig. 1*B*) and assessed

their luciferase reactivation activity (Fig. 1*C*). Incorporation of Hsp104 subunits into Hsp104[A503V] hexamers caused a shallow curvilinear decline in luciferase disaggregase activity consistent with ~4–5 WT Hsp104 subunits being necessary to inactivate the Hsp104[A503V] hexamer (Fig. 1*C*, compare *blue markers* with *purple* and *light blue lines*). If four WT subunits inactivate the Hsp104[A503V] hexamer, then two A503V subunits are not enough for activity (hence, we need three), and if five WT subunits inactivate the Hsp104[A503V] hexamer, then a single A503V subunit is insufficient for activity (hence, we need two). Thus, 2–3 Hsp104[A503V] subunits/hexamer are required to dissolve disordered luciferase aggregates in the absence of Hsp70. Strikingly, we previously demonstrated that two Hsp104 subunits must be capable of interacting with Hsp70 to enable Hsp104-mediated disaggregation of luciferase in the presence of Hsp70 (61). Hence, it is interesting that at least two A503V subunits were needed to enable otherwise WT hexamers to disaggregate luciferase in the absence of Hsp70 (Fig. 1*C*). This finding indicates that A503V subunits might mimic the conformation of Hsp70-activated, WT Hsp104 subunits. Moreover, this dose-response curve (Fig. 1*C*) also suggests that Hsp104[A503V] subunits do not stimulate the activity of adjacent WT Hsp104 subunits (26, 62). Thus, a single Hsp104[A503V] subunit is unable to potentiate an otherwise WT hexamer.

Interestingly, however, none of the theoretical curves exactly match the experimental data (Fig. 1*C*). Rather, the data fall mostly between the curves for four or five WT subunits being required to inhibit the activity of an Hsp104[A503V] hexamer (Fig. 1*C*, compare *blue markers* with *purple* and *light blue lines*). However, we could model the observed behavior more precisely if we imposed rules whereby a WT subunit represses the activity of an adjacent A503V subunit by a factor of ~0.3 and is inactive if adjacent to another WT subunit (Fig. 1*D*, compare *blue markers* with *purple line*; see "Experimental Procedures").

Hsp104[A503V] Disaggregase Activity Is Diminished by Mutations That Disrupt Substrate Binding to NBD Pore Loops—We next examined how Hsp104[A503V] would respond to specific defects in substrate binding. Residues Tyr-257 and Tyr-662 are located in flexible pore loops located within each NBD and face the central channel through which substrate is translocated (Fig. 1*A*) (37, 38, 42–44). Each pore loop tyrosine engages substrate directly, and mutating these residues to alanine results in severely reduced (Y257A) or abolished (Y662A) disaggregation activity (43, 44). We introduced missense mutations Y257A, Y662A, or both in combination with A503V, resulting in Hsp104[Y257A/A503V], Hsp104[Y662A/A503V], and Hsp104[Y257A/A503V/Y662A]. First, we measured the ATPase activity of these Hsp104 variants using the more sensitive low salt conditions of Hattendorf and Lindquist (52), which maximally stabilize Hsp104 hexamers.

Under these conditions, surprisingly, Hsp104[A503V] displays only ~18% higher ATPase activity than Hsp104 (Fig. 2*A*). Thus, enhanced ATPase activity of Hsp104[A503V] compared with Hsp104 determined previously at physiological salt concentrations may reflect slight variations in hexamer stability (62, 77, 78). Hsp104 displayed ATPase activity similar to that of Hsp104[Y257A] and Hsp104[Y662A], but Hsp104[Y257A/Y662A] ATPase activity was significantly elevated (Fig. 2*A*). We had not observed this increase previously at physiological salt concentrations (26). Compared with Hsp104[A503V], Hsp104[Y257A/A503V] and Hsp104[Y662A/A503V] had very similar ATPase activity, whereas Hsp104[Y257A/A503V/Y662A] was ~35% lower (Fig. 2*A*). Thus, the double pore loop mutation had opposite effects on ATPase activity in the wild type *versus* A503V background (Fig. 2*A*). Nonetheless, all pore-loop variants displayed robust ATPase activity under these conditions.

We next assessed the reactivation of luciferase trapped in disordered aggregates in the absence of Hsp70 and Hsp40 but in the presence of ATP. Under these conditions, Hsp104[A503V] was ~33-fold more active than Hsp104 (Fig. 2*B*). In the A503V background, the pore loop mutations abolished this enhanced activity and reduced refolding activity to a low level similar to Hsp104 (Fig. 2*B*) (23). The effect of Y662A was slightly greater than Y257A, but either mutation severely diminished Hsp104[A503V] activity (Fig. 2*B*). Thus, Hsp104[A503V] disaggregase activity is likely mediated via substrate interactions with Tyr-257 and Tyr-662.

In the presence of 1:1 mixtures of ATP and ATPγS, Hsp104 can disaggregate disordered aggregates in the absence of Hsp70 (26, 60, 61, 68). Under these conditions, Hsp104[A503V] displays reduced luciferase reactivation activity compared with Hsp104 (Fig. 2*C*). This finding suggests that Hsp104[A503V] responds differently from Hsp104 to mixtures of ATP and ATPγS, which we explore further below. In these conditions, Hsp104[Y257A] and Hsp104[Y662A] are devoid of luciferase reactivation activity. Likewise, all pore-loop variants bearing the A503V mutation showed diminished luciferase reactivation activity (Fig. 2*C*).

Next, we studied Hsp104 disaggregase activity in the presence of Hsp72 (an Hsp70) and Hdj1 (an Hsp40). Here, Hsp104[A503V] luciferase-refolding activity was ~2-fold lower than that of Hsp104 (Fig. 2*D*). This result was surprising because Hsp104[A503V] has increased luciferase reactivation activity in the presence of Hsc70 and Hdj2 as well as Sse1, Ssa1, and Ydj1 (62, 67). Thus, the identity of Hsp70 and Hsp40 chaperone partners can modulate the activity of Hsp104[A503V] differently from Hsp104. For both Hsp104 and Hsp104[A503V], Y257A or Y662A greatly reduced activity (Fig. 2*D*). The Y257A mutation greatly impaired activity in both Hsp104 and Hsp104[A503V], whereas the Y662A or the Y257A/Y662A mutations abolish

---

FIGURE 1. **Hsp104 hexamers must contain 2–3 A503V subunits for enhanced disaggregase activity in the absence of Hsp70.** *A*, domain structure of Hsp104. The N-terminal domain (*purple*), NDB1 (*olive green*), MD (*orange*), NBD2 (*blue*), and the C-terminal domain (*red*) are shown. Hsp104 mutations included in this study and their functional effects are also shown. Mutations affecting substrate binding are shown in *mustard*, whereas mutations affecting ATP binding and hydrolysis are shown in *light blue*. The potentiating mutation A503V is shown in *pink*. *B*, theoretical Hsp104 heterohexamer ensembles containing 0–6 WT subunits as a function of the fraction of WT subunit present. *C*, Hsp104 was mixed in varying ratios with Hsp104[A503V] to create heterohexamer ensembles. Luciferase disaggregation and reactivation activity was assessed in the absence of Hsp70 and Hsp40. Values represent means ± S.E. (*error bars*) (*n* = 3). Theoretical curves are shown to illustrate the predicted result when 1–6 WT subunits are needed to inactivate the Hsp104[A503V] hexamer. *D*, the data plotted in *C* are replotted. Theoretical curves are shown where adjacent pairs of A503V:A503V or A503V:WT subunits confer hexamer activity, whereas adjacent WT subunits are inactive. Each adjacent A503V:A503V pair has an activity of 1/6. Adjacent A503V:WT pairs have a repressed activity (*r*), and the effects of various *r* values are depicted.
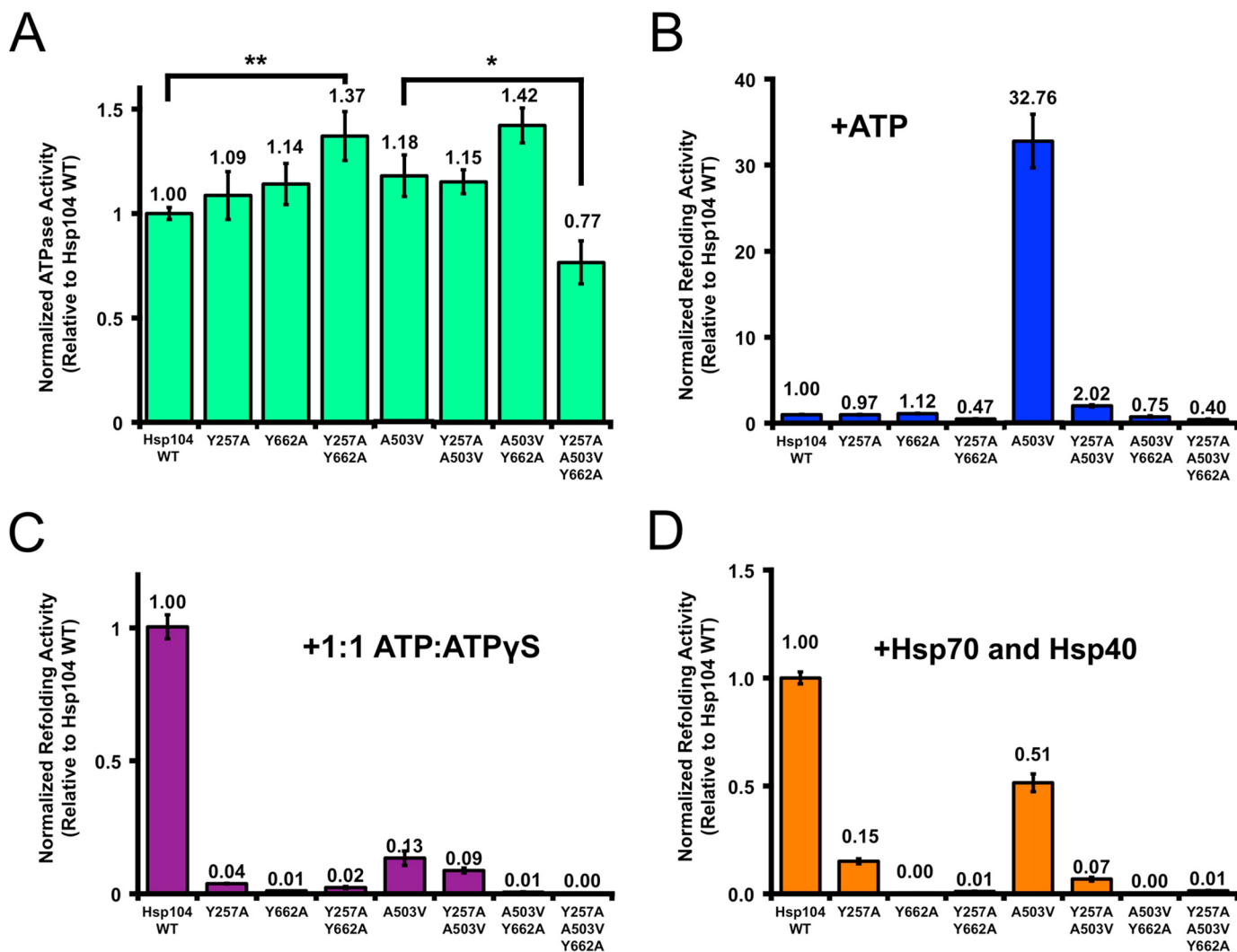
FIGURE 2. **Hsp104^{A503V} disaggregase activity is severely impaired by the Y257A mutation and ablated by the Y662A mutation.** *A*, Hsp104 mutants (0.25 μM monomer) were incubated for 10 min with ATP (1 mM). Average absorbance from a no enzyme control reaction was subtracted from raw absorbance values. The resulting absorbance values were normalized to the average absorbance yielded by Hsp104^{WT}. Values represent means $\pm$ S.E. (*error bars*) ($n = 16-48$). A one-way analysis of variance with the post hoc Tukey's multiple comparisons test (*, $p < 0.05$; **, $p < 0.01$) was performed. *B*, urea-denatured firefly luciferase aggregates were incubated for 90 min at 25 °C with Hsp104 (1 μM hexamer) plus ATP. Luciferase reactivation was then determined and normalized to Hsp104^{WT} disaggregase activity. Values represent means $\pm$ S.E. ($n = 6-90$). *C*, reactions were performed as in *B* except that 1:1 mixtures of ATP and ATPγS replaced ATP. Values represent means $\pm$ S.E. ($n = 6-84$). *D*, reactions were performed as in *B* except that Hsp70 (1 μM) and Hsp40 (1 μM) were added. Values represent means $\pm$ S.E. ($n = 6-84$).

activity (Fig. 2*D*) (62). Thus, Tyr-257 and Tyr-662 play a crucial role in Hsp104^{A503V} disaggregase activity, indicating that potentiated Hsp104 variants employ a mechanism of substrate translocation similar to that of Hsp104.

To complement our *in vitro* studies, we utilized yeast models of cytotoxic misfolding and aggregation of proteins involved in neurodegenerative diseases, such as Parkinson disease and ALS (74, 75, 79). In Parkinson disease, α-syn assembles into toxic soluble oligomers and amyloid fibrils (80). In yeast, expression of α-syn from the galactose promoter induces cytoplasmic aggregation and toxicity (79). In these experiments, we exploited a $\Delta hsp104$ yeast strain to avoid any potential interference from endogenous Hsp104 (Fig. 3, *A* and *B*) (62). Deletion or overexpression of Hsp104 does not affect α-syn aggregation or toxicity in yeast (62, 63, 67). Thus, we can be certain that any rescue of toxicity by an Hsp104 variant in the $\Delta hsp104$ background is due to a gain of Hsp104 therapeutic function (62, 63,

67). We first established that differences in growth were not due to changes in the expression of α-syn or Hsp104 variants via immunoblotting (Fig. 3*B*). As expected, a vector control, Hsp104, Hsp104^{Y257A}, Hsp104^{Y662A}, or Hsp104$^{Y257A/Y662A}$ did not reduce α-syn toxicity (Fig. 3*A*). By contrast, Hsp104^{A503V} strongly suppressed α-syn toxicity (Fig. 3*A*) (35, 62, 63, 66). This rescue was severely impaired by the Y257A mutation and ablated by the Y662A or Y257A/Y662A mutations (Fig. 3*A*).

In ALS, the RNA-binding proteins with prion-like domains, TDP-43 and FUS, mislocalize from the nucleus and form cytoplasmic aggregates in degenerating motor neurons (17, 18, 80). In yeast, expression of FUS or TDP-43 from the galactose promoter induces their cytoplasmic aggregation and toxicity (73–75). Here too, we utilized a $\Delta hsp104$ yeast strain (Fig. 3, *D–F*), in which either FUS or TDP-43 aggregates and is highly toxic (62, 73, 81). Hsp104^{A503V} mitigated cytoplasmic FUS aggregation and toxicity in yeast, whereas Hsp104 had no effect (Fig. 3*C*)
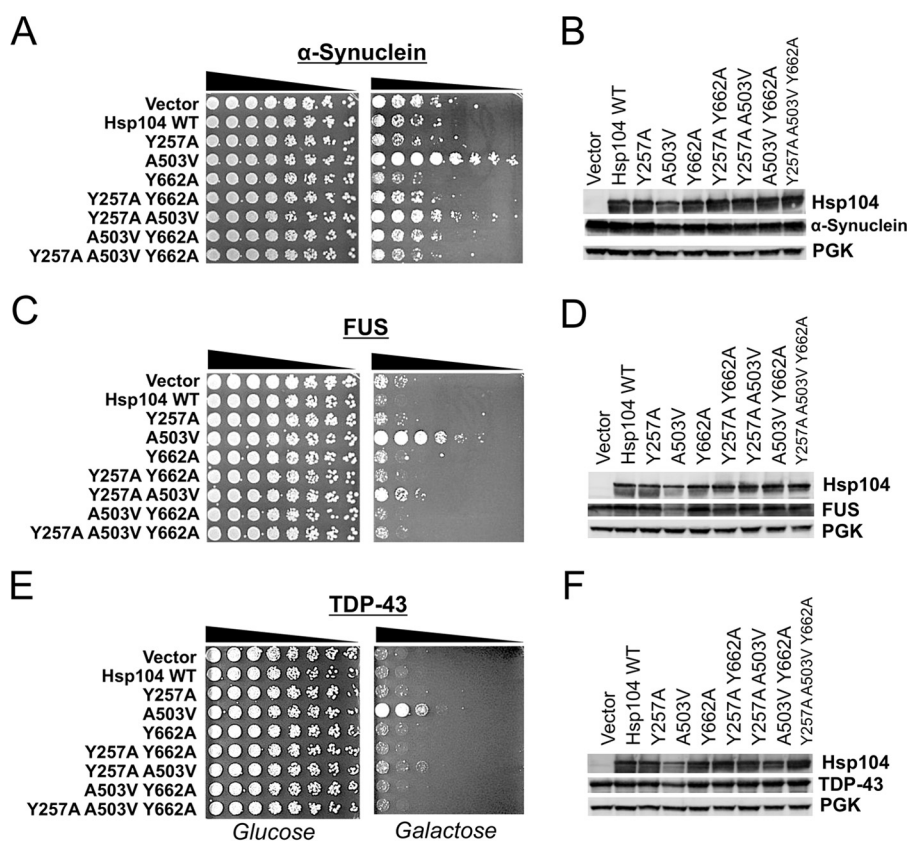
FIGURE 3. Hsp104^{A503V}-mediated rescue of yeast proteinopathy models is severely impaired by the Y257A mutation and ablated by the Y662A mutation. Δ*hsp104* yeasts integrated with genes encoding α-syn (*A*), FUS (*C*), or TDP-43 (*E*) were transformed with the indicated Hsp104 variants or empty vector control. Strains were serially diluted 5-fold and spotted on glucose (off) or galactose (on) medium. *B*, *D*, and *F*, strains from *A*, *C*, and *E*, respectively, were induced, lysed, and immunoblotted. 3-Phosphoglycerate kinase (*PGK*) was used as a loading control. Results shown are representative of at least three independent trials.

(35, 62, 63, 66, 81). This rescue was abrogated by the Y257A mutation (Fig. 3*C*). No other Hsp104 variant tested here reduced FUS toxicity (Fig. 3*C*). Consistent with previous reports (62, 63), we found that Hsp104^{A503V} slightly reduced FUS expression levels (Fig. 3*D*). However, Hsp104^{A503V} was also expressed at lower levels than the other Hsp104 variants (Fig. 3*D*).

None of the pore loop mutants could suppress TDP-43 toxicity in yeast (Fig. 3*E*) (62, 73, 74). Only Hsp104^{A503V} rescued TDP-43 toxicity (Fig. 3*E*). Hsp104^{A503V} very slightly reduced TDP-43 expression level and was itself also expressed at lower levels than Hsp104 (Fig. 3*F*). We conclude that the Hsp104 potentiation conferred by A503V is severely disrupted by the Y257A mutation and ablated by the Y662A mutation.

Hsp104^{A503V} Responds Differently from Hsp104 to Mixtures of ATP and ATPγS—Unlike Hsp104, Hsp104^{A503V} was not stimulated in luciferase reactivation by a 1:1 ratio of ATP to ATPγS in the absence of Hsp70 (Fig. 2*C*). This finding suggested that an altered pattern of ATP hydrolysis by Hsp104^{A503V} hexamers might contribute to potentiation. To explore this idea further, we examined the effect of various ratios of ATP and ATPγS on Hsp104 and Hsp104^{A503V} disaggregase activity. We kept the total adenine nucleotide concentration constant but varied the ATP/ATPγS ratio. In Fig. 4*A*, we present the data normalized to WT Hsp104 maximal activity to reveal the amplitude of the activity of the different

Hsp104 variants tested. In Fig. 4*B*, we present the data normalized to the maximal activity of each individual Hsp104 variant to reveal the optimal ATP/ATPγS ratio. Hsp104 exhibited maximal luciferase reactivation activity at ~40–50% ATPγS (Fig. 4, *A* and *B*, *blue trace*) (26, 35). By contrast, the dose response of Hsp104^{A503V} was left shifted toward lower levels of ATPγS (Fig. 4, *A* and *B*, compare *blue* and *green traces*). Thus, Hsp104^{A503V} exhibited maximal luciferase reactivation activity at ~20–30% ATPγS (Fig. 4, *A* and *B*, *green trace*) and was sharply inhibited at ATPγS concentrations that were optimal for Hsp104 (Fig. 4, *A* and *B*). Utilization of ATPγS in combination with ATP stimulates disaggregation of disordered aggregates by Hsp104 via slowing ATP hydrolysis at subset of nucleotide-binding sites (26, 60). Thus, the heightened sensitivity of Hsp104^{A503V} to stimulation by lower proportions of ATPγS indicates that Hsp104^{A503V} requires slowing of ATP hydrolysis at fewer nucleotide-binding sites than Hsp104.

ATP hydrolysis can be specifically slowed at NBD1 or NBD2 by mutating their conserved Walker A motif, which harbors a lysine residue that directly contacts the phosphates of ATP (21). Mutating the conserved lysine of the Walker A motif to threonine impairs ATP binding at that site (21, 49, 51). Alternatively, ATP hydrolysis can be slowed at NBD1 or NBD2 by mutating their conserved sensor-1 motif, which harbors a threonine or asparagine that interacts with the γ-phosphate of ATP (21, 52). Mutating the conserved threonine or asparagine of the sensor-1
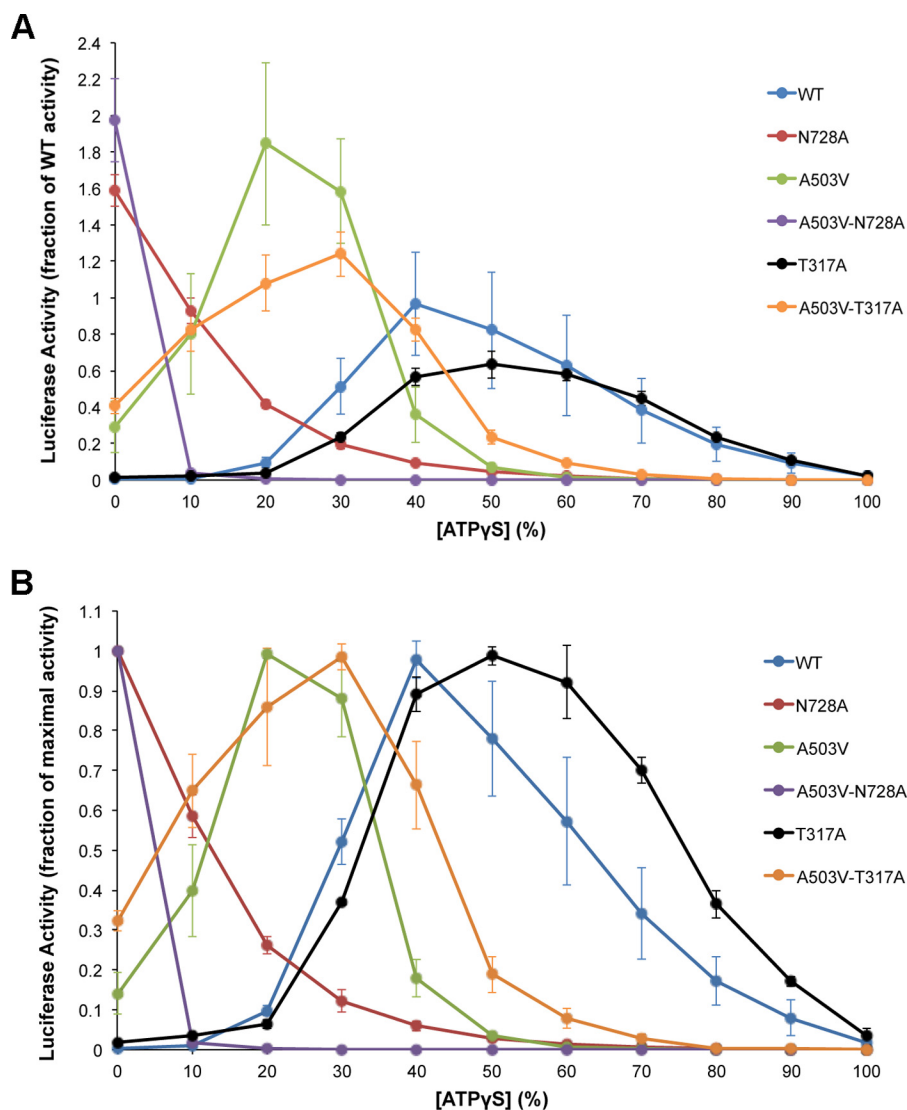
≋ASBMB

FIGURE 4. **Hsp104^{A503V} requires a lower proportion of ATPγS for maximal disaggregase activity in the absence of Hsp70 compared with Hsp104.** *A* and *B*, urea-denatured firefly luciferase aggregates were incubated for 90 min at 25 °C with the indicated Hsp104 variant (1 μM hexamer) in the presence of the indicated amounts of ATP and ATPγS (total nucleotide concentration was kept constant). Values represent means ± S.E. (*error bars*) (*n* = 4 –5). *A*, all data points were normalized to the maximum refolding activity of WT Hsp104. *B*, all data points were normalized to the maximum refolding activity for a given Hsp104 mutant.

motif to alanine does not affect ATP binding but inhibits ATP hydrolysis at that site (21, 52). Slowing ATPase activity specifically at NBD2 with K620T (Walker A) or N728A (sensor-1), but not NBD1 with K218T (Walker A) or T317A (sensor-1) (Fig. 1*A*), enables disaggregation of disordered aggregates by Hsp104 in the presence of ATP and absence of Hsp70 (Fig. 4, *A* and *B*) (data not shown) (60).

Next, we assessed how the disaggregase activity of the sensor-1 variants, Hsp104^{T317A} and Hsp104^{N728A}, was affected by increasing proportions of ATPγS. Hsp104^{T317A} showed no disaggregase activity in the presence of just ATP (Fig. 4, *A* and *B*, *black trace*) (60). Surprisingly, however, mixtures of ATP and ATPγS stimulated Hsp104^{T317A} disaggregase activity (Fig. 4, *A* and *B*, *black trace*). The dose response of Hsp104^{T317A} was similar to that of Hsp104 except slightly right-shifted toward higher ATPγS levels (Fig. 4, *A* and *B*, compare *black* and *blue traces*). Maximal Hsp104^{T317A} disaggregase activity was observed at ~50% ATPγS, and at higher ATPγS concentra-

tions, Hsp104^{T317A} disaggregase activity declined (Fig. 4, *A* and *B*, compare *black* and *blue traces*). These findings indicate that, surprisingly, slowing ATP hydrolysis at NBD2 even when it is the only intact NBD can stimulate Hsp104 disaggregase activity against disordered aggregates in the absence of Hsp70.

In striking contrast, Hsp104^{N728A} maximally reactivated luciferase in the presence of ATP but was sharply inhibited by increasing fractions of ATPγS (Fig. 4, *A* and *B*, *red trace*) (60). This finding suggests that slowing ATP hydrolysis at NBD1 when it is the only intact NBD strongly inhibits disaggregase activity against disordered aggregates in the absence of Hsp70.

Hsp104$^{T317A/A503V}$ displayed a response to ATPγS similar to that of Hsp104^{A503V} except that it was slightly right-shifted toward higher ATPγS levels (Fig. 4, *A* and *B*, compare *orange* and *green traces*). Indeed, Hsp104$^{T317A/A503V}$ was less inhibited than Hsp104^{A503V} by ATPγS at concentrations higher than 30% (Fig. 4, *A* and *B*, compare *orange* and *green traces*). Maximal Hsp104$^{T317A/A503V}$ luciferase reactivation activity was
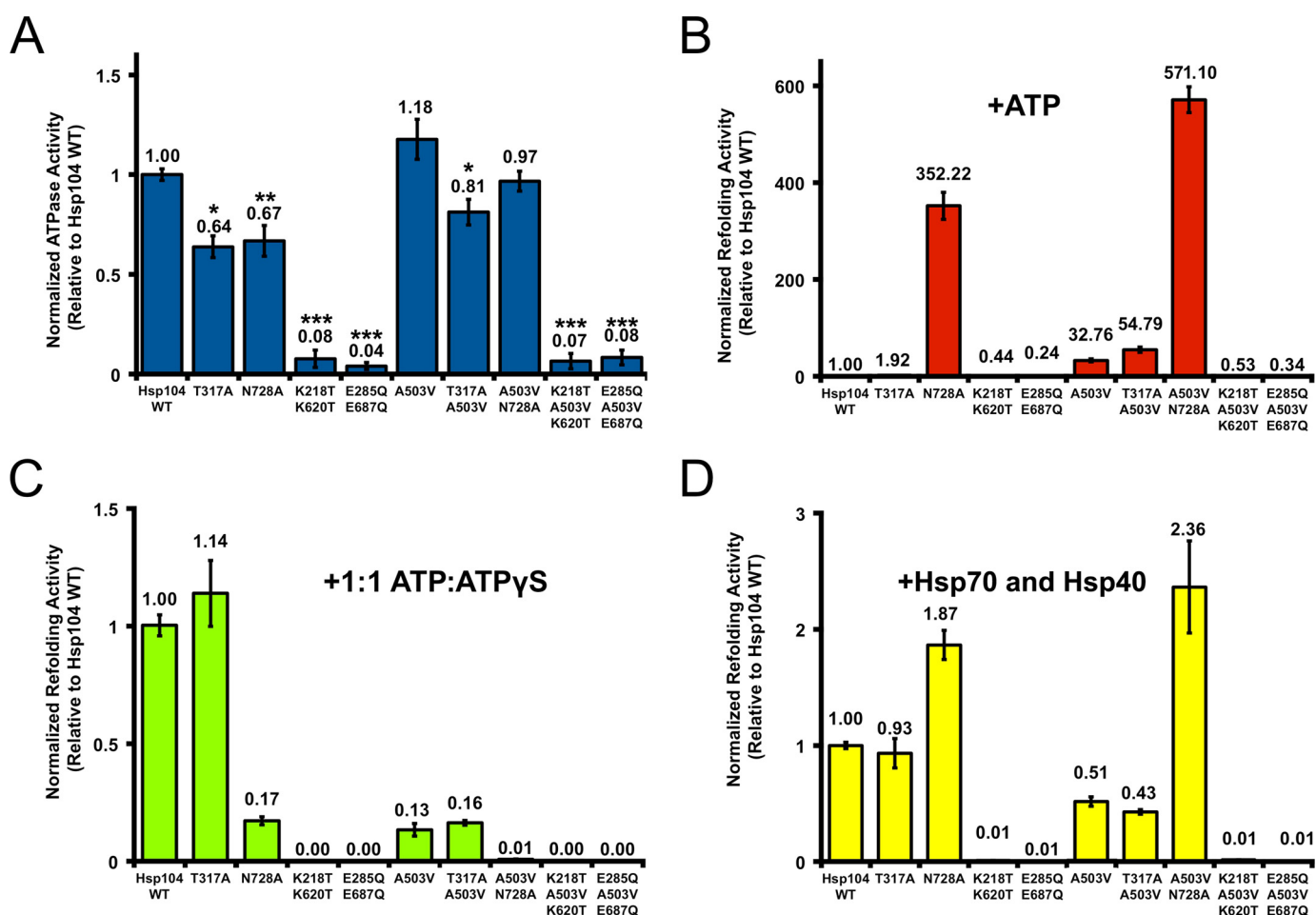
FIGURE 5. **A potentiated Hsp104 variant can overcome deficits in ATP hydrolysis at NBD1 or NBD2 *in vitro*.** *A*, Hsp104^{A503V} mutants (0.25 μM monomer) were incubated for 10 min with ATP (1 mM). Average absorbance from a no enzyme control reaction was subtracted from raw absorbance values. The resulting absorbance values were normalized to the average absorbance yielded by Hsp104^{WT}. Values represent mean ± S.E. (*error bars*) ($n = 16$–48). A one-way analysis of variance with the post hoc Tukey's multiple comparisons test (*, $p < 0.05$; **, $p < 0.01$; ***, $p < 0.001$) was performed. *B*, urea-denatured firefly luciferase aggregates were incubated for 90 min at 25 °C with Hsp104 (1 μM hexamer) plus ATP. Luciferase reactivation was then determined and normalized to Hsp104^{WT} disaggregase activity. Values represent mean ± S.E. ($n = 6$–78). *C*, reactions were performed as in *B* except that 1:1 mixtures of ATP and ATPγS replaced ATP. Values represent mean ± S.E. ($n = 6$–72). *D*, reactions were performed as in *B* except that Hsp70 (1 μM) and Hsp40 (1 μM) were added. Values represent mean ± S.E. ($n = 6$–72).

observed at ~30% ATPγS (Fig. 4, *A* and *B*, *orange trace*). Thus, the T317A mutation renders Hsp104 and Hsp104^{A503V} less sensitive to inhibition by higher ATPγS concentrations.

Remarkably, Hsp104$^{A503V/N728A}$ was even more sensitive to inhibition by ATPγS than Hsp104^{N728A} (Fig. 4, *A* and *B*, compare *purple* and *red traces*). Hsp104$^{A503V/N728A}$ maximally reactivates luciferase in the presence of ATP but is completely inhibited by as little as 10% ATPγS (Fig. 4, *A* and *B*, *purple trace*). Collectively, these observations indicate that altered ATP hydrolysis patterns might contribute to the enhanced activity of Hsp104^{A503V}. They also illustrate the startling mechanistic plasticity of the Hsp104 hexamer for disaggregating disordered aggregates (26).

Potentiated Hsp104^{A503V} Activity Can Tolerate Sensor-1 Mutations in NBD1 or NBD2—Hsp104^{A503V} exhibits increased ATPase activity at physiological salt concentrations (62, 77, 78) and is more sensitive to suramin, a small molecule inhibitor of Hsp104 ATPase activity (68). Furthermore, we show here that Hsp104^{A503V} responds differently to ATPγS (Fig. 4, *A* and *B*). Moreover, Hsp104^{A503V} ATPase activity is inhibited and not

stimulated by polylysine, unlike Hsp104 (78). These results suggest that altered ATPase activity is a key element enabling the potentiated activity of Hsp104^{A503V}. Thus, we next delineated the requirements for ATPase activity at NBD1 and NBD2 for potentiated Hsp104^{A503V} activity. To do so, we introduced the AAA+ sensor-1 mutations T317A and N728A (Fig. 1*A*) (52). We also introduced mutations in the Walker A and Walker B motifs of both NBDs; Hsp104$^{K218T/K620T}$ was unable to bind nucleotide, whereas Hsp104$^{E285Q/E687Q}$ bound nucleotide but was unable to hydrolyze it (Fig. 1*A*) (82).

In the WT Hsp104 background, both sensor-1 mutants displayed significantly reduced ATPase activity, whereas the double Walker A and Walker B mutants showed almost no activity (Fig. 5*A*) (49, 51, 52, 82). Likewise, in the A503V background, the double Walker A or double Walker B mutants eliminated ATPase activity (Fig. 5*A*). The NBD1 sensor-1 mutant displayed reduced ATPase activity in the A503V background (Fig. 5*A*; compared with Hsp104^{A503V}). Indeed, the ATPase activity of Hsp104$^{T317A/A503V}$ was reduced by ~32% compared with Hsp104^{A503V}, and this reduction was statistically significant (Fig.

5*A*). This reduction was similar to the effect of T317A in WT Hsp104 (Fig. 5*A*). By contrast, the activity of Hsp104$^{A503V/N728A}$ was reduced by only ~18% compared with Hsp104^{A503V}, and this reduction was not statistically significant (Fig. 5*A*). This reduction was not as large as the statistically significant ~33% reduction of ATPase activity caused by N728A in the WT Hsp104 background (Fig. 5*A*). However, we note that the ATPase activity of Hsp104$^{T317A/A503V}$ and Hsp104$^{A503V/N728A}$ were not significantly different (Fig. 5*A*). Collectively, these findings begin to suggest that allosteric communication between NBD1 and NBD2 may be altered in Hsp104^{A503V} (52, 78). Indeed, NBD1 appears to make a larger contribution to the ATPase activity in Hsp104^{A503V} than in Hsp104 (Fig. 5*A*). These observations indicate that NBD1 may retain high ATPase activity when NBD2 is bound with ATP in the A503V background. By contrast, in Hsp104, NBD1 ATPase activity is low when ATP is bound by NBD2 (52).

Next, we determined the luciferase disaggregase activity of these Hsp104 ATPase variants in the presence of ATP but in the absence of Hsp70. In the presence of ATP alone, the double Walker A or Walker B mutants displayed insignificant luciferase reactivation activity in both the WT and A503V backgrounds (Fig. 5*B*). As expected, Hsp104 and Hsp104^{T317A} were also inactive in this setting (Fig. 5*B*). Hsp104^{A503V} and Hsp104$^{T317A/A503V}$ displayed robust disaggregase activity under these conditions (Fig. 5*B*). Thus, reducing ATPase activity at NBD1 did not affect the ability of Hsp104^{A503V} to disaggregate disordered aggregates. Hsp104^{N728A} reactivated luciferase trapped in urea-denatured aggregates ~11-fold more effectively than Hsp104^{A503V} (Fig. 5*B*). Although Hsp104^{N728A} has previously been shown to be active under these conditions (60), we were surprised that it was considerably more active than Hsp104^{A503V}. Remarkably, Hsp104$^{A503V/N728A}$ displayed even greater luciferase reactivation activity (Fig. 5*B*). Thus, slowing ATP hydrolysis at NBD2 substantially enhances the ability of Hsp104 and Hsp104^{A503V} to disaggregate disordered aggregates in the presence of ATP and absence of Hsp70 (60).

In the presence of a 1:1 mixture of ATP/ATPγS, the double Walker A or Walker B mutants were unable to elicit any luciferase reactivation in both the WT and A503V backgrounds (Fig. 5*C*). The T317A mutation had little effect on Hsp104 activity under these conditions but slightly stimulated Hsp104^{A503V} activity (Figs. 4 and 5*C*). By contrast, the N728A mutation strongly inhibited Hsp104 and Hsp104^{A503V} activity at 1:1 ATP/ATPγS (Figs. 4 and 5*C*). Thus, slowing ATP hydrolysis at NBD2 increases the sensitivity of Hsp104 and Hsp104^{A503V} to inhibition by ATPγS.

In the presence of Hsp70 (Hsp72) and Hsp40 (Hdj1), the double Walker A or Walker B mutants were inactive in the WT and A503V background (Fig. 5*D*). Surprisingly, under these conditions, Hsp104^{T317A} activity was very similar to that of Hsp104, whereas Hsp104^{N728A} exhibited elevated activity (Fig. 5*D*). Similar results were observed in the A503V background. Thus, Hsp104$^{T317A/A503V}$ exhibited activity similar to that of Hsp104^{A503V}, whereas Hsp104$^{A503V\ N728A}$ exhibited elevated activity and was the most active variant in this assay (Fig. 5*D*). Under these conditions, slowing ATP hydrolysis at NBD2 increased Hsp104 and Hsp104^{A503V} luciferase reactivation

activity in the presence of Hsp70 and Hsp40, whereas slowing ATP hydrolysis at NBD1 had little effect on activity (Fig. 5*D*). A summary of the various activities of the Hsp104 variants tested here is presented in Table 1.

Next, we assessed whether these Hsp104 ATPase variants could rescue toxicity of α-syn, FUS, or TDP-43 in yeast (Fig. 6, *A–F*). In the context of WT Hsp104, none of the ATPase variants affected the expression or toxicity of α-syn (Fig. 6, *A* and *B*), FUS (Fig. 6, *C* and *D*), or TDP-43 (Fig. 6, *E* and *F*) in yeast. Thus, despite having enhanced ability to reactivate luciferase aggregates *in vitro* (Fig. 5, *B* and *D*), Hsp104^{N728A} was inactive against the neurodegenerative disease proteins *in vivo* (Fig. 6, *A*, *C*, and *E*). Previously, we had established that an important property of potentiated Hsp104 variants bearing mutations in the MD was increased disaggregase activity against disordered aggregates in the absence of Hsp70 and Hsp40 (62, 63, 65–67). However, our findings with Hsp104^{N728A} (Figs. 5 (*B* and *D*) and 6 (*A*, *C*, and *E*)) indicate that this activity is not sufficient for potentiated activity *in vivo*. Despite having enhanced ability to disaggregate disordered aggregates *in vitro* (Fig. 5, *B* and *D*), Hsp104^{N728A} is unable to resolve amyloid conformers (24, 33). By contrast, Hsp104^{A503V} has enhanced activity against both amyloid and non-amyloid aggregates *in vitro* (62, 63, 67). Thus, enhanced disaggregase activity against amyloid is a better predictor of potentiated activity *in vivo*.

Hsp104^{A503V} strongly rescued the toxicity of α-syn (Fig. 6*A*), FUS (Fig. 6*C*), and TDP-43 (Fig. 6*E*) in yeast (62, 63, 67). This potentiated activity was ablated by either the double Walker A or Walker B mutation (Fig. 6, *A*, *C*, *E*). Remarkably, however, both Hsp104$^{T317A/A503V}$ and Hsp104$^{A503V/N728A}$ retained potentiated activity *in vivo* and rescued toxicity of α-syn (Fig. 6*A*), FUS (Fig. 6*C*), and TDP-43 (Fig. 6*E*). Hsp104$^{T317A/A503V}$ rescued the toxicity of all three disease proteins just as well as Hsp104^{A503V} (Fig. 6, *A*, C, and *E*), whereas Hsp104$^{A503V/N728A}$ rescued α-syn and FUS toxicity just as well as Hsp104^{A503V} (Fig. 6, *A* and *C*) but had reduced ability to rescue TDP-43 toxicity (Fig. 6*E*). Rescue of α-syn toxicity was observed without any effect on α-syn expression level (Fig. 6*B*). By contrast, rescue of FUS toxicity by Hsp104^{A503V} and Hsp104$^{T317A/A503V}$ was accompanied by a reduction in FUS expression level (Fig. 6*D*). However, Hsp104$^{A503V/N728A}$ rescued FUS toxicity without affecting the FUS expression level (Fig. 6*D*). Hence, the reduction of FUS expression is not required to rescue toxicity. For TDP-43, Hsp104^{A503V} and Hsp104$^{T317A/A503V}$ also modestly reduced TDP-43 expression level, whereas Hsp104$^{A503V/N728A}$ did not (Fig. 6*F*). Therefore, the reduction in TDP-43 expression is also not required for rescue of toxicity. These findings suggest that the potentiated activity of Hsp104^{A503V} in yeast is largely unaffected by reducing ATPase activity at NBD1 or NBD2.

Discussion

Several missense mutations at specific but disparate positions in the MD or the small domain of NBD1 result in potentiated Hsp104 variants, able to dissolve protein aggregates implicated in neurodegenerative diseases (35, 62–67). These mutations probably disrupt a fragilely constrained, autoinhibited state of Hsp104 (67). However, the exact molecular

TABLE 1

Summary of Hsp104 variants and their ATPase and luciferase reactivation activities under the conditions tested in this paper

Numbers for partial or increased activities are noted. Numbers in blue represent a decrease in activity with respect to Hsp104[WT], whereas numbers in red represent increased activity.

Hsp104 Mutant	ATPase Activity	Refolding Activity		
		ATP	1:1 ATP/ATPγS	Hsp72+ Hdj1
WT	1.00	1.00	1.00	1.00
Y257A	1.09	0.97	0.04	0.15
T317A	0.64	1.92	1.14	0.93
A503V	1.18	32.76	0.13	0.51
Y662A	1.14	1.12	0.01	0.00
N728A	0.67	352.22	0.17	1.87
K218T K620T (DWA)	0.08	0.44	0.00	0.01
E285Q E687Q (DWB)	0.04	0.24	0.00	0.01
Y257A Y662A	1.37	0.47	0.02	0.01
Y257A A503V	1.15	2.02	0.09	0.07
T317A A503V	0.81	54.79	0.16	0.43
Y662A A503V	1.42	0.75	0.01	0.00
N728A A503V	0.97	571.10	0.01	2.36
K218T A503V K620T (DWA A503V)	0.07	0.53	0.00	0.01
E285Q A503V E687Q (DWB A503V)	0.08	0.34	0.00	0.01
Y257A A503V Y662A	0.77	0.40	0.00	0.01

basis of Hsp104 potentiation remains unclear. Here, we have dissected mechanistic aspects of a potentiated Hsp104 variant, Hsp104[A503V] (35, 62–67). We have revealed how many subunits within the Hsp104 hexamer must bear a potentiating mutation to yield enhanced activity. We have also determined the ATPase and substrate-binding modalities that underpin potentiation *in vitro* and *in vivo*.

Using a mutant subunit doping strategy (26, 35, 61, 70), we have established that 2–3 subunits of an otherwise WT hexamer must bear A503V mutations to elicit enhanced disaggregase activity in the absence of Hsp70. Intriguingly, at least two Hsp104 subunits must interact with Hsp70 to enable disaggregation of disordered aggregates (61). We suggest that A503V subunits mimic the conformation of WT Hsp104 subunits that have been activated by Hsp70 binding. Hsp70 and Hsp40 are often sequestered in disease-associated aggregates, which might inhibit their function (83, 84). Thus, the ability of Hsp104[A503V] to operate without Hsp70 and Hsp40 probably contributes to enhanced activity against disease-associated substrates in yeast (62, 63, 66, 67). Nonetheless, the NBD2 sensor-1 variant, Hsp104[N728A], can disaggregate disordered aggregates (but not amyloid) *in vitro* in the absence of Hsp70 (24, 33, 60), but, in contrast to Hsp104[A503V], Hsp104[N728A] is unable to rescue α-syn, FUS, and TDP-43 toxicity in yeast. It is possible that Hsp104[N728A] ATPase activity is too low to process certain aggregated substrates *in vivo* or that there are elements inhibiting activity *in vivo* that we do not reconstitute in our *in vitro* experiments. Regardless, these findings suggest that separation from Hsp70 and Hsp40 is not the only important determinant in Hsp104 potentiation.

We show that the Hsp104 potentiation conferred by A503V is severely impaired by mutating conserved substrate-binding tyrosines to alanine. In WT Hsp104, mutating Tyr-257 and Tyr-662 to alanine results in severely reduced (Y257A) or abolished (Y662A) disaggregation activity (43, 44). This was also the case for Hsp104[A503V]. Hsp104[Y257A/A503V] retained slightly more activity than Hsp104[A503V/Y662A] in all conditions tested *in vitro*. However, the Y257A pore-loop variants are unable to rescue yeast proteinopathy models. These results suggest that Hsp104[A503V] recognizes and translocates substrates via direct contact with conserved Tyr-257 and Tyr-662 pore-loop residues in a manner similar to Hsp104.

In the absence of Hsp70, Hsp104[A503V] disaggregase activity against disordered aggregates responded differently from Hsp104 to mixtures of ATP and ATPγS. Indeed, optimal Hsp104[A503V] disaggregase activity was observed at ~4:1 ATP/ATPγS compared with ~1:1 for Hsp104. Mixtures of ATPγS and ATP stimulate disaggregation of disordered aggregates by Hsp104 via decelerating ATP hydrolysis at a subset of nucleotide-binding sites (26, 60). Thus, stimulation of disaggregase activity by lower fractions of ATPγS indicates that Hsp104[A503V] requires decelerated ATPase activity at fewer nucleotide-binding sites. This finding suggests that an altered pattern of ATP hydrolysis underlies Hsp104 potentiation.
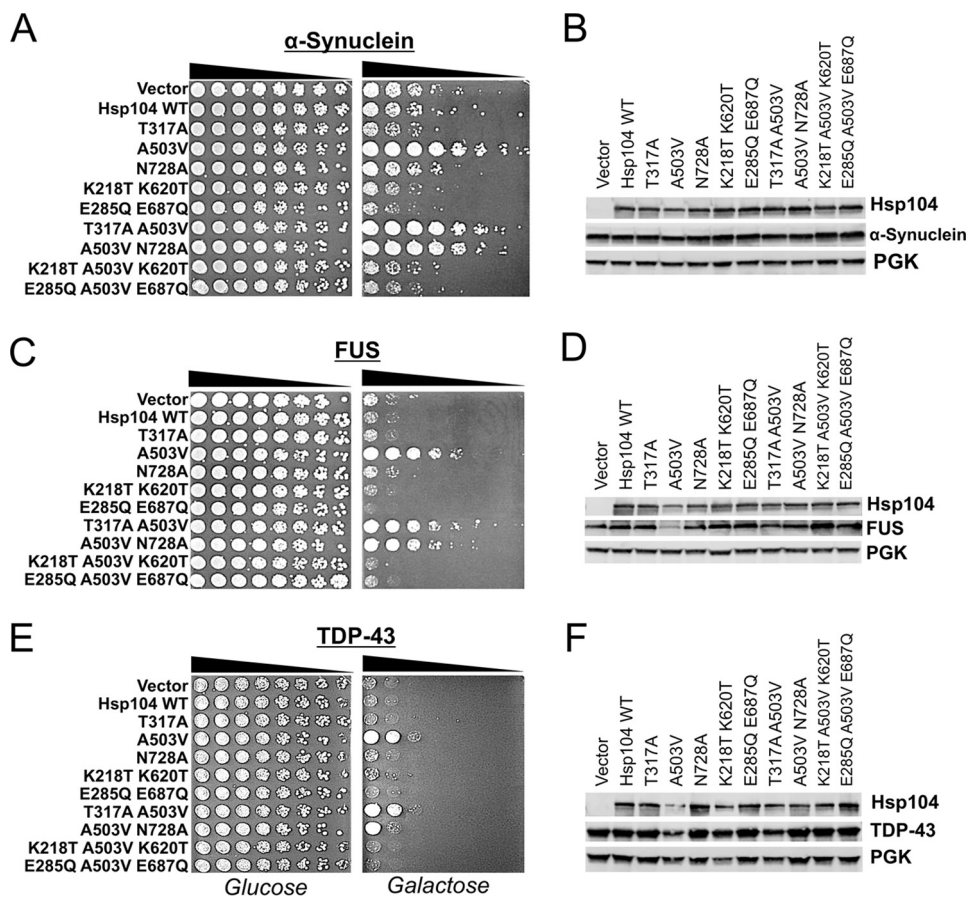
FIGURE 6. **ATPase activity at NBD1 or NBD2 in Hsp104^{A503V} is sufficient to sustain potentiation in yeast proteinopathy models.** $\Delta hsp104$ yeasts integrated with genes encoding α-syn (*A*), FUS (*C*), or TDP-43 (*E*) were transformed with the indicated Hsp104 mutants or control. Strains were serially diluted 5-fold and spotted on glucose (off) or galactose (on) medium. *B*, *D*, and *F*, strains from *A*, *C*, and *E*, respectively, were induced for 5 or 8 h, lysed, and immunoblotted. 3-Phosphoglycerate kinase was used as a loading control. Results shown are representative of at least three independent trials.
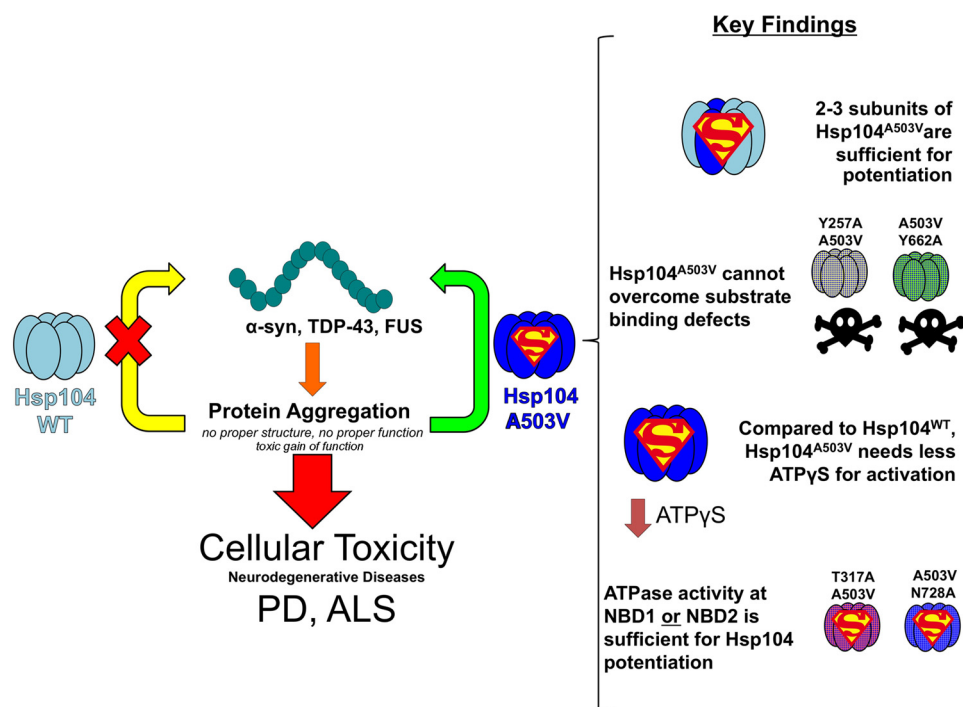

FIGURE 7. **Summary of key mechanistic insights into Hsp104 potentiation.** *PD*, Parkinson disease.

Analysis of various ATPase-defective mutants revealed that enhanced Hsp104^{A503V} activity requires ATPase activity because double Walker A or Walker B mutants were ATPase-dead and non-functional in all assays studied here (62). Interestingly, the sensor-1 mutants, T317A and N728A (52), revealed alterations in allosteric signaling between NBD1 and NBD2 in Hsp104^{A503V}. In the WT background, both T317A and N728A significantly reduce Hsp104 ATPase activity (52). Indeed, based on this observation, it is suggested that Hsp104 NBD1 ATPase activity is low when ATP is bound by NBD2 (52). However, in Hsp104^{A503V}, only the T317A mutation significantly impairs ATPase activity. Indeed, N728A has little effect on Hsp104^{A503V} ATPase activity. It should be noted that despite these differences, the ATPase activities of Hsp104$^{T317A/A503V}$ and Hsp104$^{A503V/N728A}$ were not significantly different. Nonetheless, collectively, our findings begin to suggest that NBD1 makes a larger contribution to ATPase activity in Hsp104^{A503V} than in Hsp104. The essentially unaltered ATPase activity of Hsp104$^{A503V/N728A}$ may indicate that NBD1 retains high ATPase activity when NBD2 is bound with ATP in the A503V background. We suggest that this alteration in allosteric signaling between NBD1 and NBD2 probably plays an important role in Hsp104 potentiation.

Remarkably, both Hsp104$^{T317A/A503V}$ and Hsp104$^{A503V/N728A}$ retain potentiated activity *in vivo* and *in vitro*. Thus, the potentiated activity of Hsp104^{A503V} is largely unaffected by reducing ATPase activity at NBD1 or NBD2. Hsp104$^{A503V/N728A}$ displayed slightly reduced ability to rescue TDP-43 toxicity in yeast but still provided significant rescue. By contrast, the equivalent sensor-1 mutations in WT Hsp104 greatly reduce activity in yeast with respect to thermotolerance and prion propagation (52, 85). Thus, Hsp104^{A503V} displays a more robust activity with an operational plasticity that is unperturbed by mutations that greatly reduce activity of Hsp104 *in vivo* (52, 62, 85). A summary of the key findings of our study is presented in Fig. 7.

These insights into the molecular underpinnings of Hsp104 potentiation help to lay foundations to further develop next generation Hsp104 variants with ameliorated therapeutic utility for neurodegenerative diseases. For example, our findings hint that the specificity of potentiated Hsp104 variants might be sharpened by more subtle alterations to the NBD1 pore-loop or by more severely reducing NBD2 ATPase activity. Potentiated Hsp104 variants with enhanced substrate or conformer selectivity might exhibit reduced off-target effects and consequently display increased therapeutic efficacy and safety (66).

Author Contributions—M. P. T. conceived and coordinated the study; designed, performed, and analyzed the experiments shown in Figs. 2, 3, 4, 5, and 6; generated Figs. 1*A* and 7; and wrote the manuscript. E. C. designed, performed, and analyzed the experiments shown in Figs. 2, 4, and 5. M. M. N. performed and analyzed the experiments shown in Figs. 3 and 6. M. E. J. conceived, designed, performed, and analyzed the experiment shown in Fig. 1, *B–D*, and prepared reagents used in Figs. 2, 4, and 5. M. S. G. contributed essential unpublished data, analysis, and interpretation for Fig. 2. J. S. conceived, coordinated, and directed the study and wrote the paper. All authors reviewed the results and approved the final version of the manuscript.

References

1. Höppener, J. W., Ahrén, B., and Lips, C. J. (2000) Islet amyloid and type 2 diabetes mellitus. *N. Engl. J. Med.* **343,** 411–419
2. Kaniuk, N. A., Kiraly, M., Bates, H., Vranic, M., Volchuk, A., and Brumell, J. H. (2007) Ubiquitinated-protein aggregates form in pancreatic beta-cells during diabetes-induced oxidative stress and are regulated by autophagy. *Diabetes* **56,** 930–939
3. Capellari, S., Strammiello, R., Saverioni, D., Kretzschmar, H., and Parchi, P. (2011) Genetic Creutzfeldt-Jakob disease and fatal familial insomnia: insights into phenotypic variability and disease pathogenesis. *Acta Neuropathol.* **121,** 21–37
4. Prusiner, S. B. (1998) The prion diseases. *Brain Pathol.* **8,** 499–513
5. Forman, M. S., Trojanowski, J. Q., and Lee, V. M. (2004) Neurodegenerative diseases: a decade of discoveries paves the way for therapeutic breakthroughs. *Nat. Med.* **10,** 1055–1063
6. Ross, C. A., and Poirier, M. A. (2004) Protein aggregation and neurodegenerative disease. *Nat. Med.* **10,** S10–S17
7. Lansbury, P. T., and Lashuel, H. A. (2006) A century-old debate on protein aggregation and neurodegeneration enters the clinic. *Nature* **443,** 774–779
8. Spillantini, M. G., Schmidt, M. L., Lee, V. M., Trojanowski, J. Q., Jakes, R., and Goedert, M. (1997) α-Synuclein in Lewy bodies. *Nature* **388,** 839–840
9. Dawson, T. M., and Dawson, V. L. (2003) Molecular pathways of neurodegeneration in Parkinson's disease. *Science* **302,** 819–822
10. Luk, K. C., Kehm, V., Carroll, J., Zhang, B., O'Brien, P., Trojanowski, J. Q., and Lee, V. M. (2012) Pathological α-synuclein transmission initiates Parkinson-like neurodegeneration in nontransgenic mice. *Science* **338,** 949–953
11. Mahul-Mellier, A. L., Vercruysse, F., Maco, B., Ait-Bouziad, N., De Roo, M., Muller, D., and Lashuel, H. A. (2015) Fibril growth and seeding capacity play key roles in α-synuclein-mediated apoptotic cell death. *Cell Death Differ.* **22,** 2107–2122
12. Lashuel, H. A., Hartley, D., Petre, B. M., Walz, T., and Lansbury, P. T., Jr. (2002) Neurodegenerative disease: amyloid pores from pathogenic mutations. *Nature* **418,** 291
13. Robberecht, W., and Philips, T. (2013) The changing scene of amyotrophic lateral sclerosis. *Nat. Rev. Neurosci.* **14,** 248–264
14. Fang, Y. S., Tsai, K. J., Chang, Y. J., Kao, P., Woods, R., Kuo, P. H., Wu, C. C., Liao, J. Y., Chou, S. C., Lin, V., Jin, L. W., Yuan, H. S., Cheng, I. H., Tu, P. H., and Chen, Y. R. (2014) Full-length TDP-43 forms toxic amyloid oligomers that are present in frontotemporal lobar dementia-TDP patients. *Nat. Commun.* **5,** 4824
15. Feiler, M. S., Strobel, B., Freischmidt, A., Helferich, A. M., Kappel, J., Brewer, B. M., Li, D., Thal, D. R., Walther, P., Ludolph, A. C., Danzer, K. M., and Weishaupt, J. H. (2015) TDP-43 is intercellularly transmitted across axon terminals. *J. Cell Biol.* **211,** 897–911
16. Kao, P. F., Chen, Y. R., Liu, X. B., DeCarli, C., Seeley, W. W., and Jin, L. W. (2015) Detection of TDP-43 oligomers in frontotemporal lobar degeneration-TDP. *Ann. Neurol.* **78,** 211–221
17. King, O. D., Gitler, A. D., and Shorter, J. (2012) The tip of the iceberg: RNA-binding proteins with prion-like domains in neurodegenerative disease. *Brain Res.* **1462,** 61–80
18. Li, Y. R., King, O. D., Shorter, J., and Gitler, A. D. (2013) Stress granules as crucibles of ALS pathogenesis. *J. Cell Biol.* **201,** 361–372
19. Neumann, M., Sampathu, D. M., Kwong, L. K., Truax, A. C., Micsenyi, M. C., Chou, T. T., Bruce, J., Schuck, T., Grossman, M., Clark, C. M., McCluskey, L. F., Miller, B. L., Masliah, E., Mackenzie, I. R., Feldman, H., Feiden, W., Kretzschmar, H. A., Trojanowski, J. Q., and Lee, V. M. (2006) Ubiquitinated TDP-43 in frontotemporal lobar degeneration and amyotrophic lateral sclerosis. *Science* **314,** 130–133

20. Mackenzie, I. R., Rademakers, R., and Neumann, M. (2010) TDP-43 and FUS in amyotrophic lateral sclerosis and frontotemporal dementia. *Lancet Neurol.* **9,** 995–1007

21. Hanson, P. I., and Whiteheart, S. W. (2005) AAA+ proteins: have engine, will work. *Nat. Rev. Mol. Cell Biol.* **6,** 519–529

22. DeSantis, M. E., and Shorter, J. (2012) Hsp104 drives "protein-only" positive selection of Sup35 prion strains encoding strong [PSI(+)]. *Chem. Biol.* **19,** 1400–1410

23. Glover, J. R., and Lindquist, S. (1998) Hsp104, Hsp70, and Hsp40: a novel chaperone system that rescues previously aggregated proteins. *Cell* **94,** 73–82

24. Shorter, J., and Lindquist, S. (2004) Hsp104 catalyzes formation and elimination of self-replicating Sup35 prion conformers. *Science* **304,** 1793–1797

25. Shorter, J. (2008) Hsp104: a weapon to combat diverse neurodegenerative disorders. *Neurosignals* **16,** 63–74

26. DeSantis, M. E., Leung, E. H., Sweeny, E. A., Jackrel, M. E., Cushman-Nick, M., Neuhaus-Follini, A., Vashist, S., Sochor, M. A., Knight, M. N., and Shorter, J. (2012) Operational plasticity enables Hsp104 to disaggregate diverse amyloid and nonamyloid clients. *Cell* **151,** 778–793

27. Parsell, D. A., Kowal, A. S., Singer, M. A., and Lindquist, S. (1994) Protein disaggregation mediated by heat-shock protein Hsp104. *Nature* **372,** 475–478

28. Vashist, S., Cushman, M., and Shorter, J. (2010) Applying Hsp104 to protein-misfolding disorders. *Biochem. Cell Biol.* **88,** 1–13

29. Sweeny, E. A., and Shorter, J. (2015) Mechanistic and structural insights into the prion-disaggregase activity of Hsp104. *J. Mol. Biol.* 10.1016/j.jmb.2015.11.016

30. Duennwald, M. L., Echeverria, A., and Shorter, J. (2012) Small heat shock proteins potentiate amyloid dissolution by protein disaggregases from yeast and humans. *PLoS Biol.* **10,** e1001346

31. Lo Bianco, C., Shorter, J., Régulier, E., Lashuel, H., Iwatsubo, T., Lindquist, S., and Aebischer, P. (2008) Hsp104 antagonizes α-synuclein aggregation and reduces dopaminergic degeneration in a rat model of Parkinson disease. *J. Clin. Invest.* **118,** 3087–3097

32. Shorter, J. (2011) The mammalian disaggregase machinery: Hsp110 synergizes with Hsp70 and Hsp40 to catalyze protein disaggregation and reactivation in a cell-free system. *PLoS One* **6,** e26319

33. Shorter, J., and Lindquist, S. (2006) Destruction or potentiation of different prions catalyzed by similar Hsp104 remodeling activities. *Mol. Cell* **23,** 425–438

34. Parsell, D. A., Kowal, A. S., and Lindquist, S. (1994) *Saccharomyces cerevisiae* Hsp104 protein: purification and characterization of ATP-induced structural changes. *J. Biol. Chem.* **269,** 4480–4487

35. Sweeny, E. A., Jackrel, M. E., Go, M. S., Sochor, M. A., Razzo, B. M., DeSantis, M. E., Gupta, K., and Shorter, J. (2015) The Hsp104 N-terminal domain enables disaggregase plasticity and potentiation. *Mol. Cell* **57,** 836–849

36. Wendler, P., Shorter, J., Plisson, C., Cashikar, A. G., Lindquist, S., and Saibil, H. R. (2007) Atypical AAA+ subunit packing creates an expanded cavity for disaggregation by the protein-remodeling factor Hsp104. *Cell* **131,** 1366–1377

37. Carroni, M., Kummer, E., Oguchi, Y., Wendler, P., Clare, D. K., Sinning, I., Kopp, J., Mogk, A., Bukau, B., and Saibil, H. R. (2014) Head-to-tail interactions of the coiled-coil domains regulate ClpB activity and cooperation with Hsp70 in protein disaggregation. *Elife* **3,** e02481

38. Wendler, P., Shorter, J., Snead, D., Plisson, C., Clare, D. K., Lindquist, S., and Saibil, H. R. (2009) Motor mechanism for protein threading through Hsp104. *Mol. Cell* **34,** 81–92

39. Lee, S., Sielaff, B., Lee, J., and Tsai, F. T. (2010) CryoEM structure of Hsp104 and its mechanistic implication for protein disaggregation. *Proc. Natl. Acad. Sci. U.S.A.* **107,** 8135–8140

40. Shorter, J., and Lindquist, S. (2005) Navigating the ClpB channel to solution. *Nat. Struct. Mol. Biol.* **12,** 4–6

41. Weibezahn, J., Tessarz, P., Schlieker, C., Zahn, R., Maglica, Z., Lee, S., Zentgraf, H., Weber-Ban, E. U., Dougan, D. A., Tsai, F. T., Mogk, A., and Bukau, B. (2004) Thermotolerance requires refolding of aggregated proteins by substrate translocation through the central pore of ClpB. *Cell* **119,** 653–665

42. Tessarz, P., Mogk, A., and Bukau, B. (2008) Substrate threading through the central pore of the Hsp104 chaperone as a common mechanism for protein disaggregation and prion propagation. *Mol. Microbiol.* **68,** 87–97

43. Lum, R., Niggemann, M., and Glover, J. R. (2008) Peptide and protein binding in the axial channel of Hsp104: insights into the mechanism of protein unfolding. *J. Biol. Chem.* **283,** 30139–30150

44. Lum, R., Tkach, J. M., Vierling, E., and Glover, J. R. (2004) Evidence for an unfolding/threading mechanism for protein disaggregation by *Saccharomyces cerevisiae* Hsp104. *J. Biol. Chem.* **279,** 29139–29146

45. Castellano, L. M., Bart, S. M., Holmes, V. M., Weissman, D., and Shorter, J. (2015) Repurposing Hsp104 to antagonize seminal amyloid and counter HIV infection. *Chem. Biol.* **22,** 1074–1086

46. Li, T., Weaver, C. L., Lin, J., Duran, E. C., Miller, J. M., and Lucius, A. L. (2015) *Escherichia coli* ClpB is a non-processive polypeptide translocase. *Biochem. J.* **470,** 39–52

47. DeSantis, M. E., and Shorter, J. (2012) The elusive middle domain of Hsp104 and ClpB: location and function. *Biochim. Biophys. Acta* **1823,** 29–39

48. Franzmann, T. M., Czekalla, A., and Walter, S. G. (2011) Regulatory circuits of the AAA+ disaggregase Hsp104. *J. Biol. Chem.* **286,** 17992–18001

49. Schirmer, E. C., Queitsch, C., Kowal, A. S., Parsell, D. A., and Lindquist, S. (1998) The ATPase activity of Hsp104, effects of environmental conditions and mutations. *J. Biol. Chem.* **273,** 15546–15552

50. Grimminger-Marquardt, V., and Lashuel, H. A. (2010) Structure and function of the molecular chaperone Hsp104 from yeast. *Biopolymers* **93,** 252–276

51. Schirmer, E. C., Ware, D. M., Queitsch, C., Kowal, A. S., and Lindquist, S. L. (2001) Subunit interactions influence the biochemical and biological properties of Hsp104. *Proc. Natl. Acad. Sci. U.S.A.* **98,** 914–919

52. Hattendorf, D. A., and Lindquist, S. L. (2002) Cooperative kinetics of both Hsp104 ATPase domains and interdomain communication revealed by AAA sensor-1 mutants. *EMBO J.* **21,** 12–21

53. Narayanan, S., Walter, S., and Reif, B. (2006) Yeast prion-protein, sup35, fibril formation proceeds by addition and substraction of oligomers. *Chembiochem* **7,** 757–765

54. Liu, Y. H., Han, Y. L., Song, J., Wang, Y., Jing, Y. Y., Shi, Q., Tian, C., Wang, Z. Y., Li, C. P., Han, J., and Dong, X. P. (2011) Heat shock protein 104 inhibited the fibrillization of prion peptide 106–126 and disassembled prion peptide 106–126 fibrils *in vitro*. *Int. J. Biochem. Cell Biol.* **43,** 768–774

55. Shorter, J., and Lindquist, S. (2008) Hsp104, Hsp70 and Hsp40 interplay regulates formation, growth and elimination of Sup35 prions. *EMBO J.* **27,** 2712–2724

56. Sweeny, E. A., and Shorter, J. (2008) Prion proteostasis: Hsp104 meets its supporting cast. *Prion* **2,** 135–140

57. Torrente, M. P., and Shorter, J. (2013) The metazoan protein disaggregase and amyloid depolymerase system: Hsp110, Hsp70, Hsp40, and small heat shock proteins. *Prion* **7,** 457–463

58. Cashikar, A. G., Duennwald, M., and Lindquist, S. L. (2005) A chaperone pathway in protein disaggregation: Hsp26 alters the nature of protein aggregates to facilitate reactivation by Hsp104. *J. Biol. Chem.* **280,** 23869–23875

59. Haslbeck, M., Miess, A., Stromer, T., Walter, S., and Buchner, J. (2005) Disassembling protein aggregates in the yeast cytosol: the cooperation of Hsp26 with Ssa1 and Hsp104. *J. Biol. Chem.* **280,** 23861–23868

60. Doyle, S. M., Shorter, J., Zolkiewski, M., Hoskins, J. R., Lindquist, S., and Wickner, S. (2007) Asymmetric deceleration of ClpB or Hsp104 ATPase activity unleashes protein-remodeling activity. *Nat. Struct. Mol. Biol.* **14,** 114–122

61. DeSantis, M. E., Sweeny, E. A., Snead, D., Leung, E. H., Go, M. S., Gupta, K., Wendler, P., and Shorter, J. (2014) Conserved distal loop residues in the Hsp104 and ClpB middle domain contact nucleotide-binding domain 2 and enable Hsp70-dependent protein disaggregation. *J. Biol. Chem.* **289,** 848–867

62. Jackrel, M. E., DeSantis, M. E., Martinez, B. A., Castellano, L. M., Stewart, R. M., Caldwell, K. A., Caldwell, G. A., and Shorter, J. (2014) Potentiated Hsp104 variants antagonize diverse proteotoxic misfolding events. *Cell*

156, 170–182

63. Jackrel, M. E., and Shorter, J. (2014) Potentiated Hsp104 variants suppress toxicity of diverse neurodegenerative disease-linked proteins. *Dis. Model. Mech.* **7,** 1175–1184

64. Jackrel, M. E., Tariq, A., Yee, K., Weitzman, R., and Shorter, J. (2014) Isolating potentiated Hsp104 variants using yeast proteinopathy models. *J. Vis. Exp.* **93,** e52089

65. Jackrel, M. E., and Shorter, J. (2014) Reversing deleterious protein aggregation with re-engineered protein disaggregases. *Cell Cycle* **13,** 1379–1383

66. Jackrel, M. E., and Shorter, J. (2015) Engineering enhanced protein disaggregases for neurodegenerative disease. *Prion* **9,** 90–109

67. Jackrel, M. E., Yee, K., Tariq, A., Chen, A. I., and Shorter, J. (2015) Disparate mutations confer therapeutic gain of Hsp104 function. *ACS Chem. Biol.* **10,** 2672–2679

68. Torrente, M. P., Castellano, L. M., and Shorter, J. (2014) Suramin inhibits Hsp104 ATPase and disaggregase activity. *PLoS One* **9,** e110115

69. Sweeny, E. A., DeSantis, M. E., and Shorter, J. (2011) Purification of hsp104, a protein disaggregase. *J. Vis. Exp.* 10.3791/3190

70. Werbeck, N. D., Schlee, S., and Reinstein, J. (2008) Coupling and dynamics of subunits in the hexameric AAA+ chaperone ClpB. *J. Mol. Biol.* **378,** 178–190

71. Moreau, M. J., McGeoch, A. T., Lowe, A. R., Itzhaki, L. S., and Bell, S. D. (2007) ATPase site architecture and helicase mechanism of an archaeal MCM. *Mol. Cell* **28,** 304–314

72. Sanchez, Y., and Lindquist, S. L. (1990) HSP104 required for induced thermotolerance. *Science* **248,** 1112–1115

73. Johnson, B. S., McCaffery, J. M., Lindquist, S., and Gitler, A. D. (2008) A yeast TDP-43 proteinopathy model: exploring the molecular determinants of TDP-43 aggregation and cellular toxicity. *Proc. Natl. Acad. Sci. U.S.A.* **105,** 6439–6444

74. Johnson, B. S., Snead, D., Lee, J. J., McCaffery, J. M., Shorter, J., and Gitler, A. D. (2009) TDP-43 is intrinsically aggregation-prone, and amyotrophic lateral sclerosis-linked mutations accelerate aggregation and increase toxicity. *J. Biol. Chem.* **284,** 20329–20339

75. Sun, Z., Diaz, Z., Fang, X., Hart, M. P., Chesi, A., Shorter, J., and Gitler, A. D. (2011) Molecular determinants and genetic modifiers of aggregation and toxicity for the ALS disease protein FUS/TLS. *PLoS Biol.* **9,** e1000614

76. Gietz, R. D., and Schiestl, R. H. (2007) High-efficiency yeast transformation using the LiAc/SS carrier DNA/PEG method. *Nat. Protoc.* **2,** 31–34

77. Schirmer, E. C., Homann, O. R., Kowal, A. S., and Lindquist, S. (2004) Dominant gain-of-function mutations in Hsp104p reveal crucial roles for the middle region. *Mol. Biol. Cell* **15,** 2061–2072

78. Cashikar, A. G., Schirmer, E. C., Hattendorf, D. A., Glover, J. R., Ramakrishnan, M. S., Ware, D. M., and Lindquist, S. L. (2002) Defining a pathway of communication from the C-terminal peptide binding domain to the N-terminal ATPase domain in a AAA protein. *Mol. Cell* **9,** 751–760

79. Outeiro, T. F., and Lindquist, S. (2003) Yeast cells provide insight into α-synuclein biology and pathobiology. *Science* **302,** 1772–1775

80. Cushman, M., Johnson, B. S., King, O. D., Gitler, A. D., and Shorter, J. (2010) Prion-like disorders: blurring the divide between transmissibility and infectivity. *J. Cell Sci.* **123,** 1191–1201

81. Ju, S., Tardiff, D. F., Han, H., Divya, K., Zhong, Q., Maquat, L. E., Bosco, D. A., Hayward, L. J., Brown, R. H., Jr., Lindquist, S., Ringe, D., and Petsko, G. A. (2011) A yeast model of FUS/TLS-dependent cytotoxicity. *PLoS Biol.* **9,** e1001052

82. Schaupp, A., Marcinowski, M., Grimminger, V., Bösl, B., and Walter, S. (2007) Processing of proteins by the molecular chaperone Hsp104. *J. Mol. Biol.* **370,** 674–686

83. Yu, A., Shibata, Y., Shah, B., Calamini, B., Lo, D. C., and Morimoto, R. I. (2014) Protein aggregation can inhibit clathrin-mediated endocytosis by chaperone competition. *Proc. Natl. Acad. Sci. U.S.A.* **111,** E1481–E1490

84. Auluck, P. K., Chan, H. Y., Trojanowski, J. Q., Lee, V. M., and Bonini, N. M. (2002) Chaperone suppression of α-synuclein toxicity in a *Drosophila* model for Parkinson's disease. *Science* **295,** 865–868

85. Takahashi, A., Hara, H., Kurahashi, H., and Nakamura, Y. (2007) A systematic evaluation of the function of the protein-remodeling factor Hsp104 in [PSI+] prion propagation in *S. cerevisiae* by comprehensive chromosomal mutations. *Prion* **1,** 69–77

Mechanistic Insights into Hsp104 Potentiation

Mariana P. Torrente, Edward Chuang, Megan M. Noll, Meredith E. Jackrel, Michelle S. Go and James Shorter

Access the most updated version of this article at doi: 10.1074/jbc.M115.707976

Alerts:
- When this article is cited
- When a correction for this article is posted

Click here to choose from all of JBC's e-mail alerts

This article cites 85 references, 30 of which can be accessed free at
http://www.jbc.org/content/291/10/5101.full.html#ref-list-1